Proceedings of DETC'02
ASME 2002 Design Engineering Technical Conferences
and Computers and Information in Engineering Conference
Montreal, Canada, September 29-October 2, 2002

DETC2002/MECH-34349

WORKSPACE-BASED ARCHITECTURE SELECTION OF A 3-DEGREE-OF-FREEDOM PLANAR PARALLEL MANIPULATOR

Imtehaze Heerah, Bongsoo Kang, James K. Mills and Beno Benhabib
Department of Mechanical and Industrial Engineering
University of Toronto
5 King's College Road, Toronto, Ontario, Canada M5S 3G8
imtehaze@mie.utoronto.ca, kang@mie.utoronto.ca, mills@mie.utoronto.ca,
beno@mie.utoronto.ca

ABSTRACT

This paper presents the workspace-based architecture selection process and singularity analysis of a high-speed, high-precision three degree-of-freedom (3-DOF) planar parallel manipulator for wire-bonding and electronic-component placement applications. A novel concept of manipulator "effective base area" is utilized for selecting the optimal architecture amongst the possible six well-known configurations. Dexterity regions, based on the manipulator requirements, within the reachable workspace have been identified for the selected architecture. Singular configurations of the optimal 3-PRR architecture have also been examined within the reachable workspace. Simulation results for both workspace and singularity analyses are also presented.

INTRODUCTION

Parallel manipulators are characterized by a closed-loop kinematic structure, while serial ones have an open-loop architecture. Development of parallel manipulators originated as early as in the 1940's by Gough [1] and in the 1960's by Stewart [2]. However, extensive research in this field began only about two decades ago, exploring their properties and commercial application potential. Parallel mechanisms have been proven to be advantageous over serial ones in several fields: High axis acceleration, high payload capacity, high mechanical rigidity and low moving inertia are among the most significant benefits of the closed-loop architectures. Serial manipulators are disadvantaged by the high moving inertia of the system, which limits their maximum acceleration, and the propagation of positioning errors due to axes being stacked on one another [3]. From this perspective, parallel mechanisms provide prospective solutions to achieve high accelerations and high positional accuracy in high-speed pick-and-place and positioning tasks.

Closed-loop architectures do however exhibit some limitations. Limited working volumes and singularities within the working volume are the main disadvantages of parallel mechanisms. Hence, it is essential to consider a performance index with respect to the workspace and singularity issues while selecting the manipulator kinematic structure. Numerous researchers have worked on specific parallel manipulator designs in the past, focusing on workspace analyses [4-6] and singularity analyses [7-9] (based on the rank deficiency of the Jacobian matrix of closed-loop architectures). The works of Gosselin and Angeles on a 3-RRR mechanism [4] and of Cleary and Arai on a modified version of the Stewart platform [9] are such examples. Yet there has been limited effort with respect to the comparison of parallel architectures (e.g., [10]).

Herein, it is proposed to design a 3-DOF planar parallel manipulator for electronic-component placement and wire bonding tasks. As such, it is crucial to approach the architecture selection problem carefully since it is well known that the reachable workspace is architecture dependent. Hence, a workspace-based comparison between the six 3-DOF planar parallel architectures has been carried out. Singularities within the reachable workspace of the selected architecture have also been investigated. The methodology adopted for the selection process involves the systematic elimination of architectures that do not fit within the established design selection criteria, namely, fixed actuators, a high global workspace to effective base area ratio, end-effector dexterity and avoidance of singular configurations within the workspace.

MANIPULATOR REQUIREMENTS

There exist three fundamental stages in pick-and-place operations, namely: Picking or placing of components (along the z-axis), positioning in the x-y directions and orientation along the z-axis.

Copyright © 2002 by ASME

Downloaded From: https://proceedings.asmedigitalcollection.asme.org on 06/28/2019 Terms of Use: http://www.asme.org/about-asme/terms-of-use

The platform, developed in our laboratory, is required to move a component-placement head in the x, y and ϕ directions (ϕ being a rotation about the z-axis) over an approximate task area of 400x400 mm^2 at high accelerations (>10g) and with high precision (<1.0 μ m). As such, the active joints will be fixed to the base in order to maintain minimal moving inertia to achieve the predefined acceleration and positional accuracy. Moreover, the moving platform is required to have an orientation range of up to 180^o.

3-DOF PLANAR PARALLEL ARCHITECTURES

Symmetrical three degree-of-freedom (3-DOF) planar parallel manipulators are made up of three identical kinematic chains and each chain has three 1-DOF joints. A typical kinematic chain is connected on one side to the ground (or a fixed base) and on the other extremity to the end effector (or moving platform). Each chain has one active joint (actuated) and two passive joints (not actuated). Several such architectures are thus possible. Given that there are three joints per kinematic chain and that each joint of the planar manipulator can be either of a prismatic or revolute nature, it can be shown that there exist eight possible arrangements. Merlet [11] has listed seven out of the eight possible architecture configurations. The eighth arrangement is infeasible due to dependency of the passive joints (of PP type) when the actuator is locked. Moreover, in order to achieve low moving inertia, the active joints must be fixed to the base. Thus, only the RRR, RPR, RRP, PRR, PPR and PRP architectures remain as the six possible configurations for the planar parallel manipulator.

The mobility, m, of the six architectures was investigated using Grubler's formula [12] for mobility before proceeding with the different analyses:

$$m = 3(l - n - 1) + \sum_{i=1}^{n} d_i \ , \qquad (1)$$

where l denotes the total number of rigid bodies of the mechanism, n refers to the total number of joints and d_i represents the number of DOF of joint i. When the actuators are locked, the mobility of all the architectures considered is *0* and with the actuators unlocked, the mobility is *3*, hence, fulfilling a general mobility criterion for 3-DOF planar parallel manipulators.

WORKSPACE ANALYSIS

Limited workspace stands as one of the primary disadvantages of parallel manipulators. As such, an appropriate workspace analysis constitutes an essential step in designing this class of manipulators, as underlined by Gosselin [13]. Architecture selection is often based on the manipulator's workspace as principal consideration together with other design issues such as accuracy, repeatability, speed and acceleration. A generic definition of the workspace of the planar manipulator is "the area that the centre of the moving platform can occupy, with at least one orientation of the end-effector." The following sections further detail the workspace analysis approach utilized in our work.

Methodology

Gosselin [4] proposed a general algorithm for the determination of the workspace of parallel manipulators, which can be summarized as follows: *finding the intersection of curves defining the boundaries of regions generated by each chain individually. Elementary portions of the region, thus formed, are then tested to determine the global workspace*. This approach is adopted in this paper as well to generate the workspaces of the different architectures investigated here. In order to ensure that the six architectures are judged in an unbiased manner, their outlining physical dimensions were kept the same. All architectures have similar fixed bases (an equilateral triangular base with sides of 792.8 mm), a moving platform (an equilateral triangle with sides of 100 mm) and a maximum reach of 600 mm for each chain. Furthermore, each active joint is fixed onto the base triangle. The six architectures - RRR, RPR, RRP, PRR, PPR and PRP - were modeled using AutoCAD v.14 and the global workspace was generated for each. Figure 1 illustrates the details of the six architectures analyzed.

Reachable Workspace and Effective Base Area

Figure 2 shows details of the reachable workspaces of the six architectures investigated. Three of the mechanisms (PRP, PPR and RRP) yield relatively small workspaces, as anticipated. Each chain of the RRP and PRP architectures has a common passive prismatic joint connected to the moving platform. This results in an additional constraint since there exists a fixed angle between the platform and each joint (Fig. 3a). The PPR architecture faces a similar problem as the angle between the first two joints of the kinematic chain (of type PP) is fixed (Fig. 3b). Parallel manipulators, in general, offer reduced workspaces due to constrained physical motion limits of each kinematic chain by the other chains. As such, an additional constraint causes a considerable decrease in the workspace for the PRP, PPR and RRP.

Although the six architectures investigated have similar footprints, the effective area required by the manipulator to operate is often quite different. One example is that of the RRR architecture that has its 'elbow' – the joint connecting the drive link and the coupler link – protruding outside the base triangle area and sweeping a bigger area than that of its fixed base. For the sake of comparison, the concept of *effective base area* is introduced as "the actual area the manipulator occupies while in operation (best fit rectangle enclosing the area swept by the moving chains)."

A ratio of the global workspace generated (G_W) to the effective base area (E_B) can further be calculated. This ratio forms a basis of comparison for the different architectures investigated. The desirable feature for selecting an architecture is a high G_W/E_B ratio, which demonstrates that the architecture has a large workspace and/or a small effective base area. The ranking order of the six architectures, considered in this paper, based on the G_W/E_B ratio, is shown in Table 1.

The six architectures were further examined for a possible trend in their ranking (as per Table 1) based on their global workspace to effective base area ratio as a result of a change in the size of the fixed base. The latter was altered while the links and moving platform parameters were kept unchanged for all architectures considered. Herein, the distance between the symmetrically-located actuators was

Copyright © 2002 by ASME

Downloaded From: https://proceedings.asmedigitalcollection.asme.org on 06/28/2019 Terms of Use: http://www.asme.org/about-asme/terms-of-use

decreased to 700 mm from 792.8 mm. The G_W/E_B ratios were evaluated for the six modified architecture configurations. These are shown in the right-hand column of Table 1. The ratios in Table 1 indicate that the RPR, PRR and the RRR architectures remain at the same ranking position as previously. The RRP and the PPR swap places while the PRP has the smallest ratio of all. The RPR, PRR and RRR kinematic structures maintain higher ratios in both cases, as illustrated by Table 1.

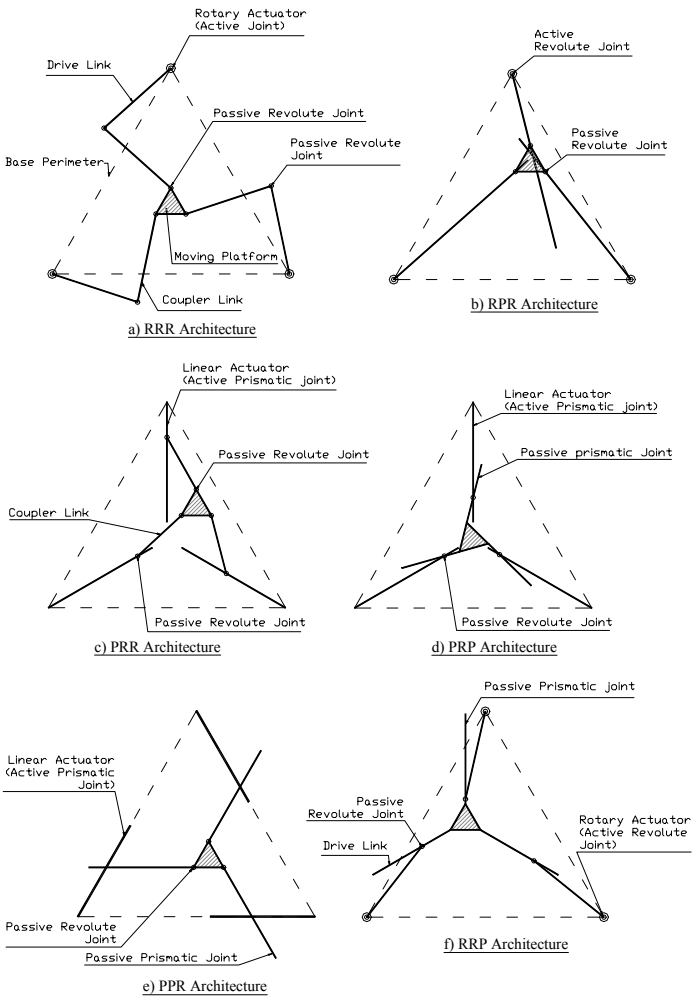

Figure 1. Parallel architecture configurations

Hence, it can be deduced that the RPR, PRR and RRR yield the best G_W/E_B relationship for 3-DOF planar parallel mechanisms with fixed active joints. Furthermore, the RPR offers the best alternative among the three mechanisms (Table 1). However, its physical implementation is not optimal: High speed and accuracy, which require low inertial loads and high rigidity of the mechanism, cannot be met by the RPR (Fig. 1b). Namely, the RPR manipulator must be implemented using a linear bearing sliding on a long shaft. Deflection of the shaft, lack of accuracy of linear bearings along length of the shaft, the requirement for uniform surface finish throughout the length of shaft and unwanted vibrations at high-speed operations, would hinder the application of this architecture for electronics applications. Thus, in our work, the PRR configuration, which is next on the ranking in Table 1 and that does not exhibit similar practical limitations as the RPR, was chosen as the optimal architecture.

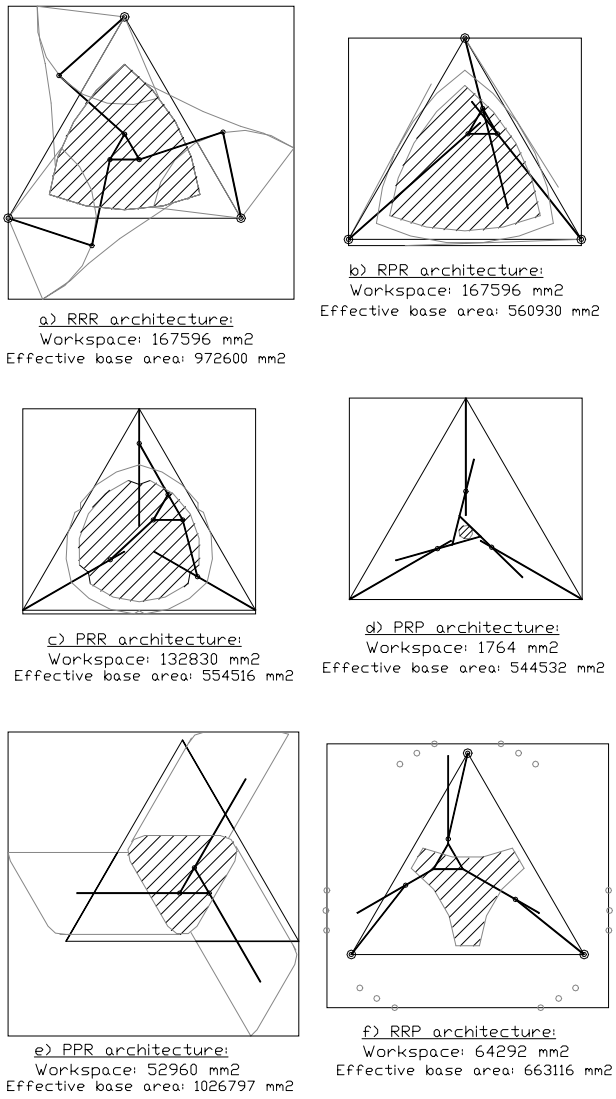

Figure 2. Workspace generated for different 3-DOF planar parallel architectures

Reachable Versus Dexterous Workspaces

The workspace considered so far is actually the global or reachable workspace - the region where the moving platform can position itself with at least one orientation. Carretero [5] defines a

Copyright © 2002 by ASME

Downloaded From: https://proceedings.asmedigitalcollection.asme.org on 06/28/2019 Terms of Use: http://www.asme.org/about-asme/terms-of-use

dexterous workspace as "*the workspace that fulfills some particular dexterity conditions, that is, the dexterity measure being smaller or equal to a particular predetermined limit*." In the current context, the *dexterity* of the moving platform (or manipulator at large) is defined as "the ability to position and orient independently." Namely, for a particular position, the moving platform of the manipulator should be able to achieve more than one orientation. The dexterous workspace of the manipulator is actually a subspace of the global workspace.

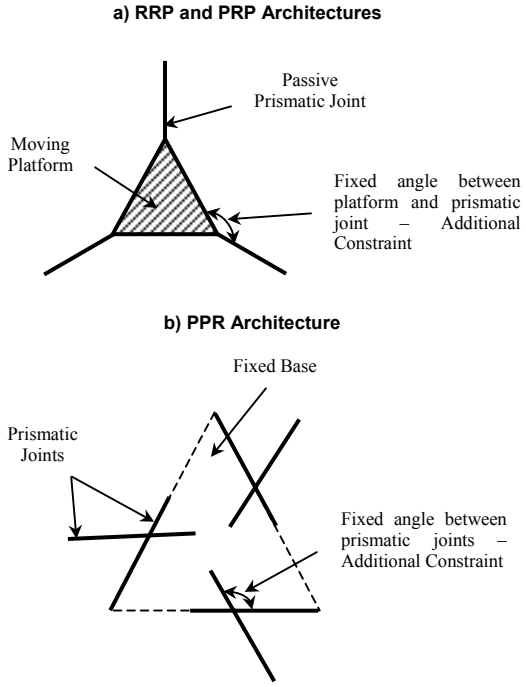

Figure 3. Additional constraints in RRP, PPR and PRP architectures

The dexterous workspace profile was determined for the selected PRR mechanism for a platform orientation ranging from 0^o to 180^o. The platform 0^o orientation here refers to the configuration where the sides of the moving platform and the fixed base triangle are parallel (Fig. 1). The 0^o orientation was chosen as starting point since the corresponding workspace area is close to that of the reachable workspace. The dexterous workspaces were determined for platform orientations of 0^o, 90^o and 180^o (Fig. 4). The choice for intervals of 90^o rests with the fact that electronic components are commonly placed orthogonal to each other on PCBs. The innermost region in Fig. 4 (representing the 180^o orientation profile) indicates the limits within which the moving platform can have any orientation varying from 0^o to 180^o.

Varying the length of the coupler links and the travel lengths of the linear actuators can further optimize the workspace. However, the modifications must ensure that the condition for elimination of voids within the workspace (length of active prismatic joint must be at least twice as long as the coupler link, i.e., $\rho_{i,\max} - \rho_{i,\min} > 2l_i$ [13]) is not violated.

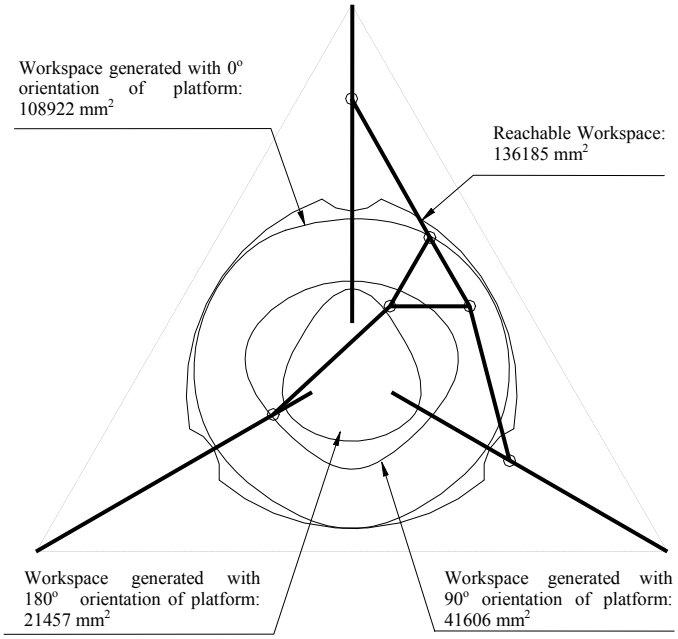

Figure 3. Dexterous workspace for the PRR architecture

SINGULARITY ANALYSIS

A singularity analysis was carried out to determine the singular configuration(s) within the global workspace. These configurations are specific poses (position and orientation) of the moving platform that result in instantaneous gain or loss of a degree of freedom, hence, causing the platform to be uncontrollable [14]. Figure 5 shows the schematic of one chain of the symmetric PRR, used for the singularity analysis.

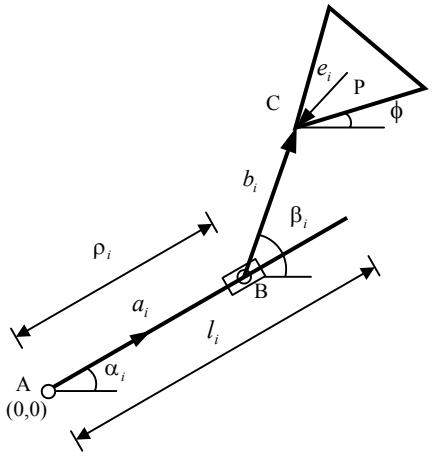

Figure 5. Schematic of a single chain for the PRR mechanism

Copyright © 2002 by ASME

Downloaded From: https://proceedings.asmedigitalcollection.asme.org on 06/28/2019 Terms of Use: http://www.asme.org/about-asme/terms-of-use

Methodology

The direct relationship between the task-space and joint space velocities for the kinematic model of the PRR architecture can be written as:

$$J_x \dot{X} + J_\rho \dot{\rho} = 0, \tag{2}$$

where $\dot{X}$ represents the set of Cartesian velocities $(\dot{x}, \dot{y}, \dot{\phi})$ of the moving platform and $\dot{\rho}$ is the set of joint velocities $(\dot{\rho}_1, \dot{\rho}_2, \dot{\rho}_3)$ - the linear velocities of the prismatic joint of the i^{th} chain of the mechanism (i=1,2,3). Also, $J_x \in R^{3x3}$ represents the direct kinematics Jacobian matrix and $J_\rho \in R^{3x3}$ is the inverse kinematics Jacobian matrix.

Singularity conditions, as in Sefrioui [7], are present whenever the determinant of J_x and/or the determinant of J_ρ is zero. For $\det(J_x)$ to be zero, there should be linear dependence of the rows/columns in the direct kinematics Jacobian matrix. In parallel, for $\det(J_\rho)$ to be zero, at least one of the diagonal elements of the inverse kinematics Jacobian should be zero. Some singular scenarios can be determined by inspection of the Jacobian matrices. Inverse kinematics singularity occurs when at least one of the coupler links is perpendicular to its respective linear actuator (that is, $a_i \perp b_i$, for i=1,2,3.). Similarly, direct kinematics singularity occurs whenever the three coupler links of the mechanism are parallel to each other $(b_1 \| b_2 \| b_3)$ or the centreline of the coupler link passes through the centre of the moving platform ($b_i \| e_i$, for i=1,2,3.). Furthermore, combined singularity can be found whenever both $\det(J_x)$ and $\det(J_\rho)$ are zero.

Simulations

The variation of the determinant of the direct kinematics Jacobian was plotted for the global workspace, for different orientations, ϕ to illustrate the various singularity scenarios. Useful features can be extracted from the plots of the determinant of the direct kinematics Jacobian against the position of the moving platform, for the predefined orientations. $\det(J_x)$ was plotted against the *x*-*y* positions of the platform for $\phi = 0, \pi/2, \pi$. The result for ϕ=0, is shown, as an example in Fig. 6. The figure reveals a singular point at the centre of the workspace of the mechanism (intersection of linear actuators travel axes) when the orientation of the platform is 0 radians. This implies that the centre of the workspace cannot be attained with a platform orientation of 0 radians, in order to avoid an uncontrollable state.

Similarly, it can be shown that no singular points exist inside the reachable workspace when the platform orientation is $\pi/2$ radians. However, the centre of the workspace is a singular point when the orientation of π radians.

Moreover, the profile of the determinant of J_x as a result of variation of the orientation of the platform for fixed positions was determined. It must be ensured that whenever the platform orientation changes (for example from 0 to $\pi/2$ radians), the mechanism is not subjected to any singularity. As an example, Fig. 7 shows the result for the case when the platform is positioned at the centre of the workspace. As shown before, $\det(J_x)$=0 when the ϕ=0. As the orientation increases (from 0 to π), the determinant also increases to a maximum at $\phi = \pi/2$ radians and drops back to zero at $\phi = \pi$ radians. It can be deduced that it is safe to operate the mechanism at the centre of the workspace for $0 < \phi < \pi$ without any risk of singularity. Likewise, different points within the global workspace can be verified for singularity as a result of a change in the orientation of the platform.

Overall, results obtained from the singularity analysis (by inspection of the Jacobian matrices, J_x and J_ρ, and by an in-depth examination of $\det(J_x)$ against platform position, *x*, *y* (Fig. 6) and orientation, ϕ (Fig. 7)) for different poses (x, y, ϕ) can eventually be grouped into a look-up singular-poses table for control tasks.

CONCLUSION

In this paper, the metrics of global workspace and effective base area have been utilized as a basis for selecting a 3-DOF planar parallel architecture. The outcome of the workspace analysis performed leads the way for effectively selecting 3 DOF planar parallel kinematic structures where main interests lie in the reachable workspace and the effective base area. The RRP, PPR and PRP architectures, as highlighted by the work carried out, are not practical mechanisms when the workspace generated is an important design criterion. The RPR, PRR and RRR are, however, feasible options and the PRR is the optimal architecture for the proposed application. A thorough analysis of the selected PRR kinematic structure has also revealed regions of dexterity for the end-effector (or moving platform). Singular configurations have been identified within the global workspace of the PRR manipulator. It is a fact that knowledge of singular conditions is of significant practical relevance. The singularity analysis results obtained in this work can, hence, be used when developing the path planning algorithm and implementing the control structure for the manipulator, thereby guaranteeing the avoidance of singular poses in practice.

ACKNOWLEDGEMENTS

This work has been supported by the Natural Sciences and Engineering Research Council of Canada (NSERC) and the first author is also grateful to the Canadian Commonwealth Scholarship and Fellowship Program (CCSFP) for its financial support.

REFERENCES

[1] Gough, V.E, 1956-1957, "Contribution to Discussion of Papers on Research in Automobile Stability, Control and Tyre Performance,"

Copyright © 2002 by ASME

Downloaded From: https://proceedings.asmedigitalcollection.asme.org on 06/28/2019 Terms of Use: http://www.asme.org/about-asme/terms-of-use

Proceedings, Auto. Division Institution of Mechanical Engineers, pp. 392-394.

[2] Stewart, D., 1965, "A Platform with Six Degrees of Freedom," Proceedings of the Institution of Mechanical Engineers, Vol. 180, No. 5, pp. 371-378.

[3] Kang, B., Chu, J., and Mills, J.K., 2001, "Design of High Speed Planar Parallel Manipulator and Multiple Simultaneous Specification Control," Proceedings, IEEE International Conference on Robotics and Automation, pp. 2723-2728.

[4] Gosselin, C.M., and Angeles, J., 1988, "The Optimum Kinematic Design of a Planar Three-Degree-Of-Freedom Parallel Manipulator," ASME Journal of Mechanisms, Transmissions and Automation in Design, Vol. 110, pp. 35-41.

[5] Carretero, J.A., Nahon, M., and Podhorodeski, R.P., 1998, "Workspace Analysis of a 3-Dof Parallel Mechanism," Proceedings, IEEE/SRJ International Conference on Intelligent Robots and Systems, pp. 1021-1026.

[6] Liu, X., Wang, J., and Gao, F., 2000, "On the Optimum Design of Planar 3-DOF Parallel Manipulators with Respect to the Workspace," Proceedings, IEEE International Conference on Robotics and Automation, pp. 4122-4127.

[7] Sefrioui, J., and Gosselin, C.M., 1992, "Singularity Analysis and Representation of Planar Parallel Manipulators," Journal of Robotics and Autonomous Systems, Vol. 10, pp. 209-224.

[8] Ma, O., and Angeles, J., 1991, "Architecture Singularities of Platform Manipulators," Proceedings, IEEE International Conference on Robotics and Automation, pp. 1542-1547.

[9] Cleary, K., and Arai, T., 1991, "A Prototype Parallel Manipulator: Kinematics, Construction, Software, Workspace Results, and Singularity Analysis," Proceedings, IEEE International Conference on Robotics and Automation, pp. 566-571.

[10] Tsai, L.W., and Joshi, S., 2001, "Comparison Study of Architectures of Four 3-Degree-Of-Freedom Translational Parallel Manipulators," Proceedings, IEEE International Conference on Robotics and Automation, pp. 1283-1288.

[11] Merlet, J.P., 1996, "Direct Kinematics of Planar Parallel Manipulators," Proceedings, IEEE International Conference on Robotics and Automation, pp. 3744-3749.

[12] Merlet, J.P., 2000, *Parallel Robots*, Kluwer Academic Publishers, Boston, MA.

[13] Gosselin, C.M., Lemieux, S., and Merlet, J.P, 1996, "A New Architecture of Planar Three-Degree-Of-Freedom Parallel Manipulator," Proceedings, IEEE International Conference on Robotics and Automation, pp. 3738-3743.

[14] Tsai, L., 1999, *Robot Analysis – The Mechanics of Serial and Parallel Manipulators*, John Wiley & Sons. Inc., New York.

Table 1. Workspace analysis results

Architecture	*Workspace, G_W/mm^2*	*Effective Base Area, E_B/mm^2*	*% G_W/E_B*	*% G_W/E_B (700 mm side base)*
RPR	167596	560930	29.9	49.4
PRR	132830	554516	23.9	42.6
RRR	167596	972600	17.2	16.7
RRP	64292	863116	7.4	3.4
PPR	52960	1026797	5.2	13.6
PRP	1764	544352	0.3	0.2

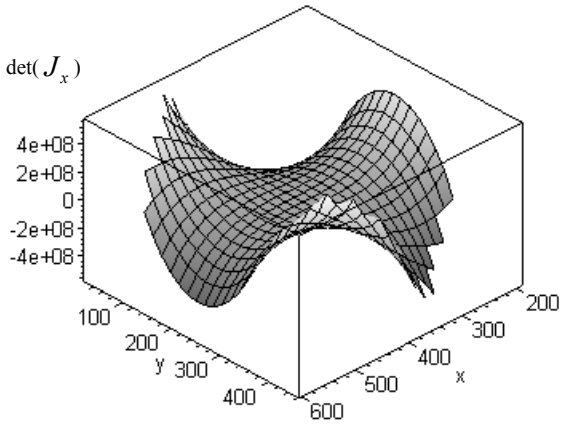

Figure 6. Variation of determinant of J_x with position of platform for ϕ = 0

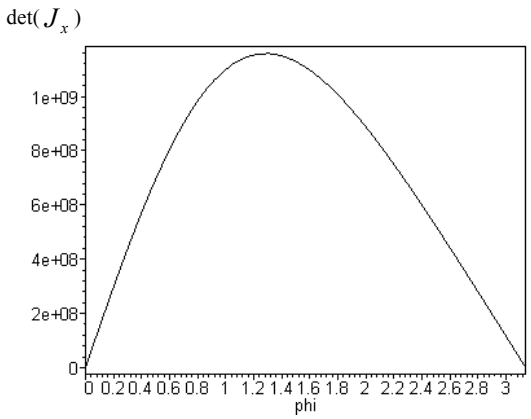

Figure 7. Variation of determinant of J_x with orientation at the center of the global workspace

Copyright © 2002 by ASME

Downloaded From: https://proceedings.asmedigitalcollection.asme.org on 06/28/2019 Terms of Use: http://www.asme.org/about-asme/terms-of-use